Estimation of radar-rainfall error spatial correlation

Villarini, Gabriele.; Smith, James A.; Mandapaka, Pradeep V.; Krajewski, Witold F.; Ciach, Grzegorz J.

2008

Mandapaka, P. V., Krajewski, W. F., Ciach, G. J., Villarini, G., & Smith, J. A. (2008). Estimation of Radar-rainfall Error Spatial Correlation. Advances in Water Resources, 32(7), 1020–1030.

https://hdl.handle.net/10356/95610

https://doi.org/10.1016/j.advwatres.2008.08.014

Estimation of Radar-Rainfall Error Spatial Correlation

by

PRADEEP V. MANDAPAKA, WITOLD F. KRAJEWSKI, GRZEGORZ J. CIACH,

GABRIELE VILLARINI,

IIHR–Hydroscience & Engineering

The University of Iowa, Iowa City, IA 52242, USA

JAMES A. SMITH

Department of Civil & Environmental Engineering

Princeton University, Princeton, NJ 08544, USA

Corresponding author address:

Pradeep V. Mandapaka

IIHR-Hydroscience & Engineering

The University of Iowa,

Iowa City, IA 52242-1585, USA

E-mail: pmandapa@engineering.uiowa.edu

Tel: 319-594-2481

Submitted to

Advances in Water Resources

July 2008

Abstract

The study presents a theoretical framework for estimating the radar-rainfall error spatial correlation (ESC) using data from relatively dense rain gauge networks. The error is defined as the difference between the radar estimate and the corresponding true areal rainfall. The method is analogous to the error variance separation that corrects the error variance of a radar-rainfall product for gauge representativeness errors. The study demonstrates the necessity to consider the area-point uncertainties while estimating the spatial correlation structure in the radar-rainfall errors. To validate the method, the authors conduct a Monte Carlo simulation experiment with synthetic fields with known error spatial correlation structure. These tests reveal that the proposed method, which accounts for the area-point distortions in the estimation of radar-rainfall ESC, performs very effectively. The authors then apply the method to estimate the ESC of the National Weather Service's standard hourly radar-rainfall products, known as digital precipitation arrays (DPA). Data from the Oklahoma Micronet rain gauge network (with the grid step of about 5 km) are used as the ground reference for the DPAs. This application shows that the radar-rainfall errors are spatially correlated with a correlation distance of about 20 km. The results also demonstrate that the spatial correlations of radar-gauge differences are considerably underestimated, especially at small distances, as the area-point uncertainties are ignored.

1. Introduction

It is widely acknowledged that radar-rainfall estimates, which serve as an input to hydrometeorological and water resource applications, are corrupted by high uncertainties that originate from many sources (e.g., Zawadzki [54], Austin [5]; Fabry et al. [20], Kitchen and Jackson [32], Hunter [29], Smith et al. [44], Steiner et al. [45], Young et al. [51], Young et al. [52], Krajewski and Smith [34], Borga [6]). Given the current state of technology, it is practically impossible to accurately measure the true area-averaged rainfall. Therefore, the quantification of radar-rainfall uncertainties (including their spatiotemporal structure) must be executed by approximating the true areal rainfall with point rainfall measurements from rain gauges. The problems associated with this approximation are well recognized (e.g., Zawadzki [53]; Austin [5]; Kitchen and Blackall [31]; Ciach and Krajewski [11] and [12]; Villarini and Krajewski [48]; Villarini et al. [49]), but are difficult to overcome (e.g., Ciach et al. [14]; Habib et al. [26]; Ciach and Krajewski [15]). A reliable methodology for the comprehensive characterization of the radar-rainfall uncertainties must start with the identification and estimation of the joint probability distribution of radar-estimated rainfall and the corresponding true rainfall over a broad range of conditions (Ciach et al. [16]). These conditions include different space and time scales, different distances from radar and rainfall regimes, and different radar systems and rainfall estimation algorithms. From the joint distribution, one can derive different synthetic characteristics of the radar rainfall errors, from the simple performance criteria (such as the root mean squared error) to the error distributional properties and its spatiotemporal dependences. Clearly, establishing such a

comprehensive methodology poses a challenge. We are confident that this challenge is surmountable, though only through many years of collaborative research. The present study constitutes another small but significant step in this direction.

A complete statistical characterization of radar-rainfall uncertainties must include the biases (e.g., Smith and Krajewski [43], Anagnostou et al. [4], Seo et al. [41], Ciach et al. [13], Borga and Tonelli [7]), the error variance (e.g., Ciach and Krajewski [11], Anagnostou et al. [3], Chumchean et al. [10]), conditional distributions of the errors (Ciach et al. [16]), and a description of the error dependences in space and time. Because correlation functions are simple expressions of these spatiotemporal error dependences, they provide a good starting point.

In their study on probabilistic quantitative precipitation estimation, Ciach et al. [16] developed a model for radar-rainfall errors, in which the relation between true rainfall and radar-rainfall is described by two elements, a deterministic distortion function and a random component. In addition to estimating the frequency distribution of the random component, they showed empirically that this component is correlated in space and time. Other radar-rainfall and satellite-rainfall error models that have been commonly used in the error propagation studies assumed either uncorrelated errors (e.g., Sharif et al. [42], Georgakakos and Carpenter [24], Carpenter and Georgakakos [8]) or considered arbitrary models of the error correlation structure (e.g., Gebremichael and Krajewski [23], Nijssen and Lettenmaier [38], Hossain et al. [28], Carpenter and Georgakakos [9], Villarini et al. [47]). However, many researchers realize that more accurate knowledge of the error correlations is crucial to the successful application of any rainfall estimate.

For example, Nijssen and Lettenmaier [38] conducted a Monte Carlo simulation experiment to assess the effects that spatial sampling errors in precipitation have on hydrological predictions. They perturbed gauge-based interpolated rainfall estimates with synthetically generated uncorrelated and correlated error fields. The perturbed rainfall fields were then used as an input to a macroscale hydrologic model. Nijssen and Lettenmaier [38] concluded that spatial correlations in the errors strongly affect predictions of hydrological fluxes and states. Hossain et al. [28], in their study on the effect of satellite-rainfall uncertainties on the flood prediction uncertainty, employed a simple multiplicative error model with temporal error correlation modeled as a lag-one autocorrelation function. While they showed that the effect of temporal error correlation is insignificant for 3-h and 6-h sampling intervals, they indicated that it might be significant at the hourly sampling interval. Carpenter and Georgakakos [9] also studied the sensitivity of ensemble flow predictions to input uncertainties. In their radar-rainfall error model, they assumed a linear spatial correlation function for the errors and concluded that the radar-rainfall error structure affects the mean areal precipitation uncertainties at the sub-catchment and watershed scales. Villarini et al. [47] studied the effects of radar-rainfall errors on the spatial scaling properties estimated from the radar-based rainfall maps. They perturbed the radar-rainfall fields with lognormally distributed multiplicative errors, assuming different levels of their spatial correlation. The study showed that the error itself has a strong effect on the scaling function of the perturbed radar-rainfall fields. However, they found that increasing the correlation level results in a decrease of the distortions in the scaling function. Based on the aforementioned literature, we argue that it is important to verify whether the radar-rainfall uncertainties

are correlated in space and, if they are, to quantify this correlation as a function of the separation distance.

The main objective of the current study is to present a practical method for estimating the radar-rainfall error spatial correlation (ESC), accounting for the area-point differences inherent in any radar-gauge comparisons. In their preliminary error correlation estimates, Ciach et al. [16] simply ignored the gauge representativeness errors. The method discussed here is conceptually analogous to the error variance separation (EVS) method proposed by Ciach and Krajewski [11]. In estimating the radar-rainfall error variance, use of the EVS procedure can account for the gauge representativeness errors. Defining the radar-rainfall error as the difference between the true areal rainfall and corresponding grid-averaged gauge rainfall, the EVS-corrected error variance is obtained by subtracting the area-point difference variance from the variance of the difference between the grid-averaged radar-rainfall and the corresponding rain gauge rainfall. The EVS method is based on the assumption that the radar and gauge errors are uncorrelated. Although in practice this zero-correlation assumption can be not fully satisfied, the EVS-corrected radar-rainfall error variance is considerably more accurate than the uncorrected error variance obtained directly from the radar-gauge pairs (Ciach et al. [14]). Many studies have employed the EVS method to characterize the variance of the radar and satellite derived rainfall products (e.g., Chumchean et al.[10], Krajewski et al. [33], Young et al. [51], Habib and Krajewski [25], Seo and Breidenbach [40], Gebremichael et al. [22], Gebremichael and Krajewski [23], Zhang et al. [55]). In the method for radar-rainfall ESC estimation presented here, we also account for the area-point differences.

The radar-rainfall uncertainties can be represented as either multiplicative or additive errors. The EVS method was originally proposed by Ciach and Krajewski [11] for the additive errors only. For this error representation, the underlying assumptions of the EVS scheme are systematically discussed in Ciach et al. [14]. For the multiplicative errors, the EVS method can be used in the logarithmic domain (Anagnostou et al. [3]). However, the possible adverse consequences of the logarithmic transformation remain unverified, which prompted us to follow the additive definition of radar-rainfall errors as in Ciach and Krajewski [11].

This paper is organized as follows: in Section 2, we derive the expression for the estimation of the radar-rainfall ESC. Section 3 describes the procedure to estimate various terms in the expression for ESC. In Section 4, we test our method for removing the area-point effects from the ESC estimates using a simulation framework. In Section 5, we apply the method to estimate ESC in the National Weather Service's operational radar-rainfall products that are provided by the precipitation processing system (PPS) of the NEXRAD in the form of the hourly digital precipitation arrays (DPA). As a ground reference for these estimates, we use the data from an experimental rain gauge network in Oklahoma known as the ARS Micronet, which is operated by the Agricultural Research Service of the United Stated Department of Agriculture. Section 6 summarizes the results and concludes this study.

2. ESC Derivation

The formula for error spatial correlation can be derived using an extension of the EVS method since we start by partitioning the variogram of the radar-rainfall. Let the radar

estimates over the two pixels 1 and 2 (Figure 1) be R_1 and R_2, respectively. The variance of the difference R_1-R_2 can be partitioned to incorporate radar-rainfall error terms as follows:

$$\begin{aligned} Var\{R_1 - R_2\} &= Var\{(R_1 - T_1) - (R_2 - T_2) + (T_1 - T_2)\} \\ &= Var\{R_1 - T_1\} + Var\{R_2 - T_2\} + Var\{T_1 - T_2\} \\ &\quad -2Cov\{R_1 - T_1, R_2 - T_2\} \\ &\quad +2Cov\{R_1 - T_1, T_1 - T_2\} \\ &\quad -2Cov\{R_2 - T_2, T_1 - T_2\} \end{aligned} \tag{1}$$

where R_1 and R_2 are radar-rainfall estimates and T_1 and T_2 are true area-averaged rainfall accumulations over the pixels 1 and 2, and operators $Var\{\cdot\}$ and $Cov\{\cdot\}$ are the variance and the correlation of the corresponding random variables. Equation (1) contains three variance terms and the three covariance terms. $Var\{R_1 - T_1\}$ and $Var\{R_2 - T_2\}$ are the variances of radar-rainfall errors over pixels 1 and 2, respectively, and $Var\{T_1 - T_2\}$ is the variogram of the true rainfall. The three covariance terms are:

1. $Cov\{R_1 - T_1, R_2 - T_2\}$ is the covariance between the radar-rainfall errors $R_1 - T_1$ and $R_2 - T_2$, i.e., the error spatial covariance.
2. $Cov\{R_1 - T_1, T_1 - T_2\}$ is the covariance between the radar-rainfall error over grid 1 and the difference $T_1 - T_2$.
3. $Cov\{R_2 - T_2, T_1 - T_2\}$ is the covariance between the radar-rainfall error over grid point 2 and the difference $T_1 - T_2$.

We assume that the covariances (2) and (3) above are equal, and hence the sum $2Cov\{R_1 - T_1, T_1 - T_2\} - 2Cov\{R_2 - T_2, T_1 - T_2\}$ in the equation 1 is equal to zero. With this assumption, equation 1 is rearranged to obtain the error spatial covariance as follows:

$$Cov\{R_1 - T_1, R_2 - T_2\} = \frac{1}{2}\left[Var\{R_1 - T_1\} + Var\{R_2 - T_2\}\right] + \frac{1}{2}\left[Var\{T_1 - T_2\} - Var\{R_1 - R_2\}\right] \quad (2)$$

The radar-rainfall error spatial covariance can be obtained by adding the following two terms: a) average of error variances at locations 1 and 2 (Figure 1) and b) difference of semivariograms of the true areal rainfall and the radar-rainfall. The error correlation can be obtained by normalizing the covariance with the product of the square root of the error variances.

3. ESC estimation

Once we derived the governing formulae, we needed to estimate the terms in (2). All four terms on the right-hand side of the equation for the ESC can be estimated directly from data.

3.1. Estimation of error variance

We employed the EVS method proposed by Ciach and Krajewski [11] to estimate the terms $Var\{R_1 - T_1\}$ and $Var\{R_2 - T_2\}$ in equation 2. According to this method,

$$Var\{R_i - T_i\} = Var\{R_i - G_i\} - Var\{G_i - T_i\}, \quad (3a)$$

i.e., the variance of the radar-rainfall error is obtained by separating the gauge-sampling error, $Var\{G_i - T_i\}$, from the overall radar-gauge variability, $Var\{R_i - G_i\}$. The latter can be obtained directly from the data:

$$Var\{R_i - G_i\} = \frac{1}{N}\sum_{t=1}^{N}\left[R_i(t) - G_i(t)\right]^2 \quad (3b)$$

where $R_i(t)$ and $G_i(t)$, respectively, are radar- and gauge-rainfall estimates for the pixel *i* at the time step *t*. Equation 3a assumes that the radar-rainfall errors ($R_i - T_i$) are uncorrelated with the rain gauge errors ($G_i - T_i$). This zero-correlation assumption and its validity have been discussed in the Introduction. In equation 3b, temporal stationarity is assumed only to increase the sample size for the estimation of the $Var\{R_i - G_i\}$. If the rain gauge network is dense enough, the proposed method can be slightly modified and applied at each time step. It should also be noted that if there is more than one gauge in a pixel, then $G_i(t)$ represents average rainfall from all the gauges in the pixel *i* at the time step *t*. With the current computational resources, simple averaging of gauge measurements can be replaced with the block kriging. However, we used simple averages for the reasons laid out in the next paragraph.

Assuming the second-order stationarity and isotropy within the areal domain and following Morrissey et al [36], the gauge-sampling error $Var\{G_i - T_i\}$ is obtained as

$$Var\{G_i - T_i\} = Var\{G\} \cdot VRF_i, \tag{3c}$$

where $Var\{G\}$ is the variance of the point-rainfall and VRF_i is the variance reduction factor for the pixel i containing the rain gauge(s), and it is obtained as follows:

$$VRF_i = \frac{1}{n^2}\sum_{j=1}^{K}\sum_{k=1}^{K}\rho(d_{j,k})\delta(j)\delta(k) - \frac{2}{nK}\sum_{j=1}^{K}\sum_{k=1}^{K}\rho(d_{j,k})\delta(j) + \frac{1}{K} + \frac{2}{K^2}\sum_{j=1}^{K-1}\sum_{k=j+1}^{K}\rho(d_{j,k}), \tag{3d}$$

The VRF is a statistic that quantifies the spatial sampling error we make in approximating an areal value with an average of a specified number of point measurements in that area (Morrissey et al. [36]). Such a theoretical framework does not exist if the areal value is estimated from block kriging. For this reason we used simple averages in the equation 3b. The sampling domain is divided into *K* grid boxes, over which the rainfall is estimated as the arithmetic mean of *n* gauges. The Kronecker delta function $\delta(j)$ denotes whether box j contains a rain gauge. The term $\rho(d_{j,k})$ represents the rainfall spatial correlation, where $d_{j,k}$ is the distance between boxes j and k. A detailed description of equation 3d is given in Morrissey et al. [36] and Krajewski et al. [33].

3.2. Estimation of variogram of true areal rainfall

The third term on the right hand side of equation 2 denotes the variogram of the true rainfall, and for a second-order stationary process it can be shown that (e.g., Cressie [17])

$$Var\{T_i - T_j\} = 2\Gamma_T(h) = 2\left[Cov_T(0) - Cov_T(h)\right] \tag{4}$$

where $Cov_T(h)$ is the covariance of the true areal rainfall over grids i and j separated by distance h, and $Cov_T(0)$ is the variance of the true rainfall. Vanmarcke [46] (Section 6.4) gives the following expression to obtain the covariance function of the local averages of a homogeneous two-dimensional random field over square areas with sides L, from the corresponding point variance and covariance function:

$$Cov\left\{T_i, T_j\right\} = Cov_T(h) = \frac{Var\{G\}}{4L^4}\left[\sum_{a=0}^{3}\sum_{b=0}^{3}(-1)^a(-1)^b\,\Delta\left(L_{xa}, L_{yb}\right)\right], \tag{5a}$$

where T_i and T_j respectively are true areal rainfall over pixels i and j (of sides L) separated by distance lag h. To achieve lags smaller than the pixel size, the pixels i and j need to be overlapping, in which case, the equation 5a can be simplified to:

$$Cov\left\{T_i, T_j\right\} = Cov_T(h) = \frac{Var\{G\}}{4L^4}\begin{bmatrix}\Delta\left(L_{x0}, L_{y0}\right) - 2\Delta\left(L_{x0}, L_{y1}\right) + \Delta\left(L_{x0}, L_{y2}\right)\\ -2\Delta\left(L_{x1}, L_{y0}\right) + 4\Delta\left(L_{x1}, L_{y1}\right) - 2\Delta\left(L_{x1}, L_{y2}\right)\\ +\Delta\left(L_{x2}, L_{y0}\right) - 2\Delta\left(L_{x2}, L_{y1}\right) + \Delta\left(L_{x2}, L_{y2}\right)\end{bmatrix}, \tag{5b}$$

In the equations 5a and 5b, L_{x0} (L_{y0}) is the distance from the end of the first grid to the beginning of the second grid along x (y) direction; L_{x1} (L_{y1}) is the distance from the beginning of the first grid to the beginning of the second grid along x (y) direction; L_{x2} (L_{y2}) is the distance from the beginning of the first grid to the end of the second grid along x (y) direction; and L_{x3} (L_{y3}) is the distance from the end of the first grid to the end of the second grid along x (y) direction. The $\Delta(\cdot,\cdot)$ function in the equation 5a is obtained as $\Delta(L_x, L_y) = (L_x L_y)^2 \cdot \gamma(L_x, L_y)$, where

$$\gamma(L_x, L_y) = \frac{4}{L_x L_y} \int_0^{L_x} \int_0^{L_y} \left(1 - \frac{l_x}{L_x}\right)\left(1 - \frac{l_y}{L_y}\right) \rho(l) dl_x dl_y, \tag{5c}$$

where l_x and l_y are the separation distances in x and y directions, with $l = \left(l_x^2 + l_y^2\right)^{1/2}$. The variance of the areal values can be obtained from the point variance using the relation:

$$Var\{T\} = Cov_T(0) = Var\{G\} \cdot \gamma(L, L), \tag{5d}$$

For further information on equations 5a through 5d, the reader is pointed to Section 6.4 of Vanmarcke [46]. The covariance and the variance of the true areal process are then plugged in equation 4 to obtain the variogram of the true areal rainfall. Equations

(3)-(5) demonstrate that the correlation function of the point rainfall (ρ) plays an important role in estimating the ESC. In this study, we employ Pearson's correlation coefficient and justify its use in Section 5, where the correlation structure of point rainfall is estimated using rain gauges from the Oklahoma Micronet.

3.3. Estimation of variogram of radar-rainfall

The fourth term within the brackets on the right hand side of equation 2 denotes variogram of the radar-rainfall, which we estimate using the classical method-of-moments estimator (e.g., Cressie [17]).

$$Var\{R_i - R_j\} = 2\Gamma_R(h) = \frac{1}{n(h)}\sum_{i,j}^{n(h)}\left[R_i - R_j\right], \tag{6}$$

where $n(h)$ is the number of data pairs separated by lag *h*. We realize that there are estimators which are more roust to the outliers in the data then the method-of-moments estimator. The estimator proposed by Cressie and Hawkins [18] ($\hat{\gamma}_{CH}$) is among the widely used. However, we did not use it in this study as it is valid only when the distribution of differences, $Z(x) - Z(x+h)$, for a particular lag *h* is Gaussian (Lark [35]). Lark [35] compared the robustness and efficiency of $\hat{\gamma}_{CH}$ along with two other robust estimators, which also assume contaminated normal model, i.e., normal distribution in the presence of outliers. The study concluded that all the three robust estimators are influenced by any departure from the assumption of normality of differences (Lark [35]).

According to the study, the classical Method-of-Moments estimator is better than any robust estimator, when the data is skewed with no outliers.

3.4. Summary of assumptions in ESC methodology

Before we apply the method on the simulated fields and on the radar-rainfall data, we summarize here, all the assumptions involved.

a) The rainfall is second-order stationary in space and time.

b) The rainfall is isotropic. If the rainfall is anisotropic, the spatial correlation function is directional and therefore the proposed methodology has to be applied for each direction resulting in different error spatial correlation functions for different directions.

c) Radar-rainfall estimates and the rain gauge measurements are unbiased.

d) The rain gauge representativeness error is not correlated with radar-rainfall error. The assumptions (c) and (d) are required by the EVS method.

4. ESC testing using Monte Carlo simulation

We begin with a Monte Carlo simulation experiment to assess the method for the error spatial correlation and the estimation procedure discussed in the previous section. The simulation framework provides us with full control over the things that real data cannot. In the simulation experiment, we can compare the error correlations retrieved from our methodology with the true error correlations known apriori. A good performance here implies that the assumptions in our methodology are reasonable and gives us the confidence to apply the ESC methodology on the real radar-rainfall data. On a square

grid of 100×100 (arbitrary units), high resolution (0.4×0.4) two-dimensional, stationary, Gaussian and lognormal processes with an exponential correlation function are generated using the circulant embedding technique (e.g., Dietrich and Newsam [19], Wood and Chan [50]). The exponential correlation function used in the study is:

$$\rho(d) = \theta_0 \exp\left[-(d/\theta_1)^{\theta_2}\right] \qquad (\theta_0 \in [-1,1], \theta_1 > 0, \theta_2 \geq 0), \tag{7}$$

where d is the distance between any two points in the field, θ_0 is the nugget effect that quantifies the measurement error near the origin and the micro scale variability of the process, θ_1 is the correlation distance defined as the distance at which the correlation drops to 1/e, and θ_2 is the shape factor that controls the shape of the function near the origin.

A total of 325 stations with inter-station spacing of 4 units in the x-direction and 8 units in the y-direction (Figure 2) sample the process from the simulated high resolution fields, which is similar to the sampling of rainfall process by the rain gauges. The high resolution fields are then averaged to obtain fields at a resolution of 4×4 as it is the most commonly used resolution for radar-rainfall data in many hydrological applications. These average fields are analogous to the true areal rainfall fields at a particular resolution. Hereafter, the high resolution and corresponding average fields are referred to as HR and true areal (TA) processes, respectively.

We do not interpret the simulated Gaussian and lognormal fields as rainfall fields. Our objective in the simulation experiment is to evaluate the methodology on simple case

of Gaussian realizations and on a complex case of lognormal fields. The ESC approach can be applied to any remotely sensed physical process that meets the criteria such as second-order stationarity and isotropy and where there are inherent area-to-point errors in the evaluation. That's the reason we labeled the process from where we sample the "point data" as high resolution (HR) process and the corresponding area averaged process as true areal (TA) process and the error corrupted fields as areal-with-error (AE) process.

The next step in the simulation framework is to generate the error process at a resolution of 4×4, assuming that they are Gaussian with zero mean, unit variance and following an exponential correlation function (equation 7) with a correlation distance of 20 distance units. Since the method is derived for additive errors, we add the error fields to the TA fields to obtain the "areal with error" (AE) process. Addition of Gaussian errors to the Gaussian (or lognormal) process results in some negative values in the AE process, which is not realistic for rainfall fields. However, this would not affect our results because our aim in this section is solely to test the method. The above procedure is repeated to obtain multiple realizations of AE fields.

We then applied the method on the simulated fields to estimate the error spatial correlation. Because the spatial correlation of the errors is known, the accuracy of our framework can be assessed by comparing the estimated and true ESC. We also compare them with spatial correlations of the difference between the 325 sampling points and corresponding AE pixels (analogous to radar-gauge difference), which we call "radar-gauge (RG)" error spatial correlation.

4.1. Gaussian realizations

We start by simulating correlated Gaussian realizations with mean zero and variance equal to 1 and we consider two correlation distances of 10.0 and 40.0 (arbitrary distance units). For both cases, the correlation functions of HR, TA, error, and the AE fields are estimated using the 325 sampled points (Figure 3). Figure 3 illustrates that the correlation structure of the high resolution process and the error process is quite accurate, which gives us confidence in the simulated fields. The variogram of the TA process obtained using the procedure described in Section 3 and that of the AE process obtained using the classical method of moments estimator are shown in Figure 4 for the two point correlation functions considered. From the TA variograms (particularly for the correlation distance of 10), one sees that the variance (half the sill) is smaller than the variance of the corresponding HR process (which is equal to 1.0). This is expected, as the TA process is obtained as an average of the HR process. From Figure 4, it is also apparent that an addition of correlated errors to the TA process increases its variance.

The error correlations obtained using our method is fitted with a three-parameter exponential function using the Levenberg-Marquardt algorithm and is compared with the spatial correlation of RG differences and that of true errors in Figure 5. It can be seen from the Figure 5 that our method can retrieve the error correlation structure quite accurately for both of the considered correlation functions. Though the correlation structure of RG differences is close to the true one, there is a consistent bias, which is quite evident for a smaller correlation distance of 10.0. This bias is due to the fact that RG differences have inherent area-point errors.

4.2. Lognormal realizations

In testing our method on the simulated lognormal realizations, we considered the same correlation functions that are used in the Gaussian case. In addition to the correlation distances, we also varied the coefficient of variation (CV) of the lognormal realizations. Therefore, for simulations with lognormal realizations, we have four different combinations of variability, as indicated in Table 1. The number of realizations used for each case is also shown in Table 1.

We obtain the lognormal process by transforming a simulated Gaussian process. However, the transformation results in the alteration of the parameters of the lognormal realizations. As our aim is to obtain lognormal process with a certain mean, variance, and correlation structure, we selected the parameters of the simulated Gaussian fields such that the transformation will lead to lognormal fields with the desired parameters.

The correlation functions of the HR, TA, error, and AE fields estimated using 325 sampling locations are plotted in Figure 6. The HR correlation functions estimated from the simulations closely match the theoretical correlation functions. The figure also reveals that as the CV increases and correlation distance decreases, the addition of the error field has little impact on the correlation function of the true areal process. Figure 7 illustrates the variograms of TA and the AE process for all combinations of correlation functions and CVs. The behavior of the TA and AE variograms for all four cases is similar to that of the Gaussian simulations with the variance of the TA process being smaller than the corresponding HR process. The ESC technique is applied on all four cases (Table 1) and is shown in Figure 8 along with the fitted three parameter exponential correlation function and correlation of RG differences. Comparing the correlations of

RG differences with the true one, a systematic underestimation can be seen from the Figure 8. This bias increases as the lognormal field becomes more variable (a high CV and small correlation distance). As in the Gaussian case, the biased RG correlations result from area-point errors. Unlike in the Gaussian case, the ESC results in a consistent bias for a larger CV and smaller correlation distance (Figure 8). Further investigation into case 4 of lognormal simulations revealed that bias in the estimation of variance reduction factor is the main reason for the systematic underestimation in ESC and, hereafter, all the results in this section are for case 4.

As mentioned in Section 3, the VRF is a theoretical framework to quantify the spatial sampling error involved in approximating an areal value with an average of point measurements within the area. For the VRF to be strictly applicable in the simulation framework, the areal values need to be obtained by averaging infinite number of point values. For the Gaussian simulations, this is not an issue as the TA value (4.0×4.0) - obtained as an average of 100 pixels of HR process (0.4×0.4) - is reasonably closer to the true areal process. Case 4 in the lognormal simulations, with a high CV and small correlation distance, is highly variable, and the 100 HR pixels are inadequate to obtain the TA process. Therefore, the VRF estimated as in equation 3d overcorrects the area-point discrepancies leading to underestimation of error correlation (Figure 8d). For the lognormal simulations, we repeat case 4 (Table 1 and Figure 8d) with the TA process obtained by averaging the HR process simulated on 0.1×0.1 grids and Figure 9 shows that the bias in ESC reduces with an increase in the resolution. Therefore, our method's systematic underestimation of error spatial correlation for lognormal realizations is

largely an artifact of the simulation experiment, and the ESC method performs well in a simulation framework.

5. Application to the Oklahoma ARS Micronet Dataset

After testing the method in the simulation framework, we applied it to estimate the ESC of NEXRAD hourly digital product (DPA) from the Oklahoma City NEXRAD (KTLX) radar site (Fulton et al. [21]). We used a high density and high quality rain gauge network, the Oklahoma Micronet, established by the Agricultural Research Service in Little Washita experimental watershed, Oklahoma (e.g., Allen and Naney [2]; Young et al. [52], Ciach et al. [14]). Figure 10 shows the network and the hydrologic rainfall analysis project (HRAP) radar grid, which is a quasi-rectangular grid with the size of the cell ranging from 3.5 km in the southern U.S. to 4.5 km in the northern U.S. (Reed and Maidment, [39]). The rain gauge network covering an area of approximately 1200 km^2, consists of 41 gauges on a fairly regular grid with intergauge distances ranging from around 3 to 40 km and the average nearest-neighbor distance of approximately 5 km. In our analysis, we considered a square radar domain with sides of 60 km, covering the rain gauge network, for a 36-month period (April-September data for six years 1998-2003), thereby reducing any seasonal effects.

The first step in applying the ESC method is to estimate the point correlation function of rainfall. Though Pearson's estimator is widely used to estimate the correlation, it has been shown in the literature that for highly skewed distributions, it results in biased estimates (e.g., Hutchinson [30], Habib et al. [27]). Assuming that the data come from the mixed lognormal distribution, Habib et al. [27] proposed an alternative unbiased

approach to estimate the correlation. To check if the lognormality assumption is valid for the Oklahoma Micronet, the rainfall data measured by the rain gauges is binned into intervals of 0.5, and a mixed lognormal distribution is fitted to this binned data. The gauge-rainfall had a lighter tail with respect to a mixed lognormal distribution. Therefore, we stick to the Pearson's estimator to obtain the point correlation function of the rainfall. Figure 11 portrays the correlation function of the rainfall measured by the rain gauges and the fitted three-parameter exponential function (Equation 7). We used this parametric form of the correlation structure to obtain the error variance and the variogram of the true areal rainfall (Equations 3 through 5). The radar pixel is nine orders of magnitude larger than the sampling area of rain gauge. Therefore, artifacts introduced by equation 3d in the estimation of VRF and subsequently the spatial correlation of errors are negligible.

The next step in the ESC method is the estimation of the variogram of the radar-rainfall. Its estimation is performed by using a classical method-of-moments estimator (Equation 6) and binning the moments into 4 km distance classes. All the pixels covering 60×60 km^2 are used in the estimation process. The size of the estimation domain and number of realizations play an important role in the estimation of variance and covariance leading to their severe underestimation. We did a systematic sensitivity study on this aspect and found that the bias decreases rapidly with the number of independent realizations (Mandapaka et al. [36]). For example, if the estimation domain is half the decorrelation distance, we found that as few as 50 independent fields would suffice to give us an unbiased estimate of variance and covariance. Since we used six years of hourly data, underestimation of variance and covariance is not an issue.

Before we proceed to use the radar data, we would like to mention that the overall mean of the Micronet gauge estimates over 36 months is equal to 0.083 mm and that of collocated radar pixels for the same time period is 0.116 mm. The bias can be treated in an additive or multiplicative manner. The former approach would result in unrealistic negative rainfall values for the radar pixels. When the latter approach is used, the variogram of the DPA estimates would be almost the same as the variogram of true areal rainfall. Our methodology (Equation 2) applied in such a situation leads to the error covariance being constant and equal to the error variance. The result is in contrast to the RG error correlations estimated from multiplicatively corrected radar fields as they decreasing with distance. Therefore, we applied the error spatial correlation approach directly on the uncorrected radar data. To make sure that the proposed methodology is robust to handle such bias we ran a simulation experiment similar to Section 4.1 but with uncorrelated errors and a bias of 0.5 to the AE fields. Despite the bias in the AE fields, the proposed methodology correctly identified the zero error correlations.

Figure 12 shows the estimated and fitted radar estimates along with the variogram of the true areal rainfall obtained using equation 4. The error variances and the variograms of the true areal and radar-rainfall are then used in the ESC method (Equation 2) to estimate the spatial covariance of errors, which when normalized with error variances, results in an error spatial correlation structure (Figure 13). The spatial correlation of the RG differences is also plotted in the same figure for comparison. From Figure 13, one notices that our method results in tighter (less scatter) correlation estimates than those obtained directly from the radar-gauge pairs that neglect the area-point errors. The decreased scatter is due to the use of parametric point correlation functions in equations 3

through 5. However, for both cases, we can infer that radar-rainfall errors are significantly correlated with a correlation distance of approximately 20 km (Figure 13). This is an important result as in most of the error propagation studies, the errors are assumed to be uncorrelated.

Further, one can observe in Figure 13 that ignoring the area-point differences results in underestimation of the ESC at the shorter distances. Though this bias is not significant at the daily and, to an extent, hourly scales for stratiform rainfall, it might be significant at the sub-hourly time scales and for the tropical regime as the rainfall becomes more variable.

6. Summary and conclusions

Defining the radar-rainfall error as the difference between the radar-estimated rainfall and the corresponding true areal rainfall, we propose a method to estimate the error spatial correlation (ESC) that accounts for the rain gauge representativeness errors. The required information on the area-point difference structure was obtained from relatively dense rain gauge networks. Although this study considered only the additive error definition, it can be applied to the multiplicative errors by transforming the variables into the logarithmic domain. Conceptually, our ESC estimation method is an extension of the error variance separation method proposed by Ciach and Krajewski [11]. After formal derivation of the method, it was tested on simulated Gaussian and lognormal fields with known ESC. It performed very well in estimating the ESC for Gaussian fields and for lognormal fields with lower coefficients of variation (CV). However, as the CV of the lognormal fields increased, our test results tended to underestimate the ESC. The fact

that this specific underestimation decreases systematically with increasing the resolution of the simulated fields shows that this effect is an artifact of the simulation caused by the finite resolution of the simulated fields. The ESC obtained using our method was also compared with the ESC obtained directly from the simulated "radar-gauge" differences. This comparison showed that ignoring the area-point errors can result in considerable underestimation of the error spatial correlation structure, especially at small separation distances.

After the computer simulation tests, the ESC method was applied to the DPA products that are the standard outcomes of the PPS in the NEXRAD. This application was based on six years of warm season (April to September) KTLX radar data, and the corresponding data from a relatively dense experimental rain gauge network (Oklahoma ARS Micronet). These results show that the radar-rainfall errors are spatially correlated and that their correlation distance is approximately 20 km. Although this application has been limited to the central Oklahoma region, it offers insight into the spatial correlation of DPA radar-rainfall errors in any region where the rainfall is mostly of stratiform and mixed form. The results in this study can be helpful for new radar-rainfall error propagation studies that account for the ESC in the radar-rainfall data. It is worth mentioning that the radar errors are dependent on location and range from the radar. However we are applying the ESC method within the 60×60 km^2 pixel assuming stationarity and isotropy. If we can have dense networks such as Micronet in different zones (distances from radar), we can estimate the error spatial correlation for each zone and for each direction using the proposed methodology. We would also like to mention that the proposed method is not conditioned on the intensity and type of precipitation.

The ESC method presented here can be extended by regarding the ESC as a dynamically varying random function for which state estimation procedures are derived. The simplest way of implementing such an extension is by treating the correlation distance of the radar-rainfall error field as a random process in time. One can include this state variable as an element of the ESC estimation problem where the updating of the state is based on the currently observed radar-rainfall fields and the corresponding rain gauge data. This extension would eliminate the need for the data to be stratified into several "seasons." It would also reflect the fact that even during the peak of the warm season, the large extratropical cyclones with prevailing areas of stratiform rainfall regime can be mixed with highly variable convective cells embedded within the stratiform rainfall fields. Our future studies will feature such an extension.

Acknowledgments

The authors acknowledge support from NSF Grants EAR-0309644, EAR-0409738, and EAR-0409501 and useful discussions with Mekonnen Gebremichael. The authors also thank two anonymous reviewers and Prof. Geoff Pegram for their comments and suggestions that led to an improved manuscript. Gabriele Villarini was supported by NASA Headquarters under the Earth Science Fellowship Grant NNX06AF23H. The second author acknowledges the support of the Rose and Joseph Summers Chair endowment.

REFERENCES

[1]. Aitchison, J., and J.A.C. Brown. The lognormal distribution with special reference to its uses in economics. University of Cambridge, Department of Applied Economics, Monograph: 5, Cambridge University Press 1957; pp. 176.

[2]. Allen, P.B., and J.W, Naney. Hydrology of the Little Washita River Watershed, Oklahoma: Data, and Analyses. United States Department of Agriculture, Agricultural Research Service, ARS-90 1991; pp. 73.

[3]. Anagnostou, E.N., W.F. Krajewski, and J.A. Smith. Uncertainty quantification of mean-areal radar-rainfall estimates. Journal of Atmospheric and Oceanic Technology 1999; 16: 206-215.

[4]. Anagnostou, E.N., W.F. Krajewski, D.-J. Seo, and E.R. Johnson. Mean-field rainfall bias studies for WSR-88D. Journal of Hydrologic Engineering 1998; 3: 149-159.

[5]. Austin, P.M. Relation between measured radar reflectivity and surface rainfall. Monthly Weather Review 1987; 115: 1053-1070.

[6]. Borga, M. Accuracy of radar rainfall estimates for streamflow simulation. Journal of Hydrology 2002; 267: 26-39.

[7]. Borga, M., and F. Tonelli. Adjustment of range dependent bias in radar rainfall estimates. Journal of Physics and Chemistry of the Earth 2000; 10: 909-914.

[8]. Carpenter, T.M., and K.P. Georgakakos. Impacts of parametric and radar rainfall uncertainty on the ensemble streamflow simulations of a distributed hydrologic model. Journal of Hydrology 2004; 298: 202-221.

[9]. Carpenter, T.M., and K.P. Georgakakos. Discretization scale dependencies of the ensemble flow range versus catchment area relationship in distributed hydrologic modeling. Journal of Hydrology 2006; 328: 242-257.

[10]. Chumchean, S., A. Sharma, and A. Seed. Radar rainfall error variance and its impact on the radar rainfall calibration, Journal of Physics and Chemistry of the Earth 2003; 28: 27-39.

[11]. Ciach, G.J., and W.F. Krajewski. On estimation of radar-rainfall error variance. Advances in Water Resources. 1999; 22: 585-595.

[12]. Ciach, G.J. and W.F. Krajewski. Radar-rain gauge comparisons under observational uncertainties. Journal of Applied Meteorology 1999; 38: 1519-1525.

[13]. Ciach, G.J., M.L. Morrissey, and W.F. Krajewski. Conditional bias in radar rainfall estimation. Journal of Applied Meteorology 2000; 39: 1941-1946.

[14]. Ciach, G.J., E. Habib, and W.F. Krajewski. Zero-covariance hypothesis in the error variance separation method of radar rainfall verification. Advances in Water Resources 2003; 26: 573-580.

[15]. Ciach, G.J., and W.F. Krajewski. Analysis and Modeling of Spatial Correlation Structure in Small-Scale Rainfall in Central Oklahoma. Advances in Water Resources 2006; 29: 1450-1463.

[16]. Ciach, G.J., W.F. Krajewski, and G. Villarini. Product-Error driven uncertainty model for probabilistic quantitative precipitation estimation with NEXRAD data. Journal of Hydrometeorology 2007; 8: 1325-1347.

[17]. Cressie, N.A.C., Statistics for Spatial Data. Wiley and Sons, 1993; pp. 462.

[18]. Cressie, N.A.C. and D.M. Hawkins, Robust estimation of the variogram, I. Journal of the International Association of Mathematical Geology, 1980; 12: 115-125.

[19]. Dietrich, C.R., and G.N. Newsam. A fast and exact method for multidimensional Gaussian stochastic simulations. Water Resources Research 1993; 29: 2861-2869.

[20]. Fabry, F., G.L. Austin, and D. Tees. The accuracy of rainfall estimates by radar as a function of range. Quarterly Journal of Royal Meteorological Society 1992; 118: 435-453.

[21]. Fulton, R.A., J.P. Breidenbach, D.-J. Seo, and D.A. Miller. The WSR-88D Rainfall Algorithm. Weather and Forecasting 1998; 13: 377-395.

[22]. Gebremichael, M., W.F. Krajewski, M.L. Morrissey, D, Langerud, G.J. Huffman, and R. Adler. Error uncertainty analysis of GPCP monthly rainfall products: A data based simulation study. Journal of Applied Meteorology 2003; 42**:** 1837-1848.

[23]. Gebremichael, M., and W.F. Krajewski. Assessment of statistical characterization of small-scale rainfall variability from radar: Analysis of TRMM ground validation datasets. Journal of Applied Meteorology 2004; 43: 1180-1199.

[24]. Georgakakos, K.P., and T.M. Carpenter. A methodology for assessing the utility of distributed model forecast applications in an operational environment, In: Tachikawa, Y., Vieux, B.E., Georgakakos, K.P., Nakakita, E. (Eds.). Weather Radar Information and Distributed Hydrological Modeling. IAHS publications No. 282. IAHS Press 2003; 85-92.

[25]. Habib, E., and W.F. Krajewski. Uncertainty analysis of TRMM ground validation radar-rainfall products: Application to the TEFLUN-B field campaign. Journal of Applied Meteorology 2002; 41: 558-572.

[26]. Habib, E., G.J. Ciach, and W.F. Krajewski. A method for filtering out raingauge representativeness errors from the verification distributions of radar and raingauge rainfall. Advances in Water Resources 2004; 27: 967-980.

[27]. Habib, E., W.F. Krajewski, and G.J. Ciach. Estimation of rainfall interstation correlation. Journal of Hydrometeorology 2001; 2: 621-629.

[28]. Hossain, F., E.N. Anagnostou, and T. Dinku. Sensitivity analysis of satellite retrieval and sampling error on flood prediction uncertainty. IEEE Transactions on Geoscience and Remote Sensing 2004; 42: 130-139.

[29]. Hunter, S.M. WSR-88D radar rainfall estimation: capabilities, limitations and potential improvements. National Weather Digest 1996; 20: 26-38.

[30]. Hutchinson, T.P. A comment on correlation in skewed distributions. Journal of General Psychology 1997; 124: 211-215.

[31]. Kitchen, M., and R.M. Blackall, Representativeness errors in comparisons between radar and gauge measurements of rainfall. Journal of Hydrology 1992; 132: 13-33.

[32]. Kitchen, M., and P.M. Jackson. Weather radar performance at long range simulated and observed. Journal of Applied Meteorology 1993; 32: 975-985.

[33]. Krajewski, W.F., G.J. Ciach, J.R. McCollum, and C. Bacotiu. Initial validation of the global precipitation climatology project monthly rainfall over the United States. Journal of Applied Meteorology 2000; 39: 1071-1086.

[34]. Krajewski, W.F., and J.A. Smith. Radar hydrology: Rainfall estimation. Advances in Water Resources 2002; 25: 1387-1394.

[35]. Lark, R. M., A Comparison of some robust estimators of variogram for use in soil survey, European Journal of Soil Science, 2000; 51: 137-157.

[36]. Mandapaka, P.V., W.F. Krajewski, G. Villarini and G.J. Ciach. Simulation based quantification of the effects of sampling on the estimation of spatial correlation structure. Submitted to Water Resources Research.

[37]. Morrissey, M.L., J.A. Maliekal, J.S. Greene, and J. Wang. The uncertainty of simple spatial averages using raingauge networks. Water Resources Research 1995; 31: 2011-2017.

[38]. Nijssen, B., and D.P. Lettenmaier. Effect of precipitation sampling error on simulated hydrological fluxes and states: Anticipating the Global Precipitation Measurement satellites. Journal of Geophysical Research 2004; 109: D02103, doi:10.1029/2003JD003497.

[39]. Reed, S.M., and D.R. Maidment. Coordinate transformations for using NEXRAD data in GIS-based hydrologic modeling. Journal of Hydrologic Engineering 1999; 4: 174-182.

[40]. Seo, D.-J., and J.P. Breidenbach. Real-time correction of spatially nonuniform bias in radar rainfall data using rain gauge measurements. Journal of Hydrometeorology 2002; 3: 93-111.

[41]. Seo, D.-J., J.P. Breidenbach, and E.R. Johnson. Real-time estimation of mean field bias in radar rainfall data. Journal of Hydrology 1999; 223: 131-147.

[42]. Sharif, H.O., F.L. Ogden, W.F. Krajewski, and M. Xue. Numerical simulations of radar rainfall error propagation. Water Resources Research 2002; 38: 10.1029/2001WR000525.

[43]. Smith, J.A., and W.F. Krajewski. Estimation of the mean field bias of radar rainfall estimates. Journal of Applied Meteorology 1991; 30: 397-412.

[44]. Smith, J.A., D.-J Seo, M. Baeck, and M. Hudlow. An intercomparison study of NEXRAD precipitation estimates. Water Resources Research 1996; 32: 2035-2045.

[45]. Steiner M, J.A. Smith, S.J. Burges, C.V. Alonso, and R.W. Darden. Effect of bias adjustment and rain gauge data quality control on radar rainfall estimation. Water Resources Research 1999; 35: 2487-2503.

[46]. Vanmarcke, E. Random Fields: Analysis and Synthesis. MIT Press 1983; p. 382.

[47]. Villarini, G., G.J. Ciach, W.F. Krajewski, K.M. Nordstrom, and V.K. Gupta. Effects of systematic and random errors on the spatial scaling properties in radar-estimated rainfall. In: Nonlinear Dynamics in Geosciences, Tsonis, A.A. & J. Elsner, Editors, Springer 2007: 37-51.

[48]. Villarini, G., and W.F. Krajewski. Empirically-based modeling of spatial sampling uncertainties associated with rainfall measurements by rain gauges. Advances in Water Resources 2008; 31: 1015-1023

[49]. Villarini, G., P.V. Mandapaka, W.F. Krajewski, and R.J. Moore. Rainfall and sampling uncertainties: A rain gauge perspective. Journal of Geophysical Research 2008; 113: D11102, doi:10.1029/2007JD009214..

[50]. Wood, A.T.A., and G. Chan. Simulation of stationary Gaussian processes in $[0; 1]^d$. Journal of Computational and Graphical Statistics 1994; 3: 409-432.

[51]. Young, C.B., B.R. Nelson, A.A. Bradley, J.A. Smith, C.D. Peters-Lidard, A. Kruger, and M.L. Baeck. An evaluation of NEXRAD precipitation estimates in complex terrain. Journal of Geophysical Research 1999; 104: 19691-19703.

[52]. Young, C.B., A.A. Bradley, W.F. Krajewski, A. Kruger, and M. L. Morrissey. Evaluating NEXRAD multisensor precipitation estimates for operational hydrologic forecasting. Journal of Hydrometeorology 2000; 1: 241-254.

[53]. Zawadzki, I. On the radar-raingauge comparison. Journal of Applied Meteorology 1975; 14: 1430-1436.

[54]. Zawadzki, I. Factors affecting the precision of radar measurements of rain, Preprints of 22nd Conference on Radar Meteorology. American Meteorological. Society, Zurich 1984; p. 251-256.

[55]. Zhang Y., T. Adams, and J.V. Bonta. Sub-pixel scale rainfall variability and the effects on separation of radar and gauge rainfall errors. Journal of Hydrometeorology 2007; 8: 1348-1363.

List of Tables

List of Figures

the **TA** variogram is obtained by integrating the variogram of the **HR** field. The distance units and the parameters of the **Err** field are the same as in Figure 2.

Figure 5: Comparison of three functions: 1) the estimated error spatial correlation (ESC) for Gaussian realizations corrected using our method, 2) the true ESC (with correlation distance of 20), and 3) the spatial correlation structure of "radar-gauge" (RG) differences. The distance units and the parameters of the **Err** field are the same as in Figure 2.

Figure 6: Correlation functions of the lognormal **HR** fields simulated, with the parameters given in Table 1 and estimated using the sampling network shown in Figure 2. The distance units and the parameters of the **Err** field are the same as in Figure 2.

Figure 7: True areal (**TA**) and "areal with errors" (**AE**) variograms of the simulated lognormal processes of Table 1. In each panel, upper and lower curves are **AE** and **TA** variograms, respectively. The **AE** variogram is estimated using all the pixels available, and the **TA** variogram is obtained by integrating the point variogram. The distance units and the parameters of the **Err** field are the same as in Figure 2.

Figure 8: Comparison of error spatial correlation (ESC) for lognormal realizations retrieved using our correction method with the true ESC and with the spatial correlation structure of "radar-gauge" (RG) differences. The distance units and the parameters of the **Err** field are the same as in Figure 2.

Figure 9: Sensitivity of ESC method to the resolution (Res) of the simulation grid. The distance units and the parameters of the **Err** field are the same as in Figure 2.

Figure 10: Map showing the location of the Oklahoma City NEXRAD (KTLX) radar site, Oklahoma Micronet, and regional topography. The radar distance marks are 50 km apart.

Figure 11: Pearson's correlation function of gauge-rainfall obtained using six years of warm season (April to September) rainfall data from Oklahoma Micronet.

Figure 12: Radar-rainfall variogram for the National Weather Service's hourly digital product over the Oklahoma Micronet. The variogram of true areal rainfall is obtained by integrating the gauge-rainfall correlation function over the 4 km pixel.

Figure 13: Comparison of error spatial correlation of the National Weather Service's hourly digital product with the spatial correlation structure of RG differences.

Tables

Table 1: The parameters used in the four simulation scenarios with lognormal HR field. The error field (**Err**) is Gaussian with zero mean and standard deviation equal to 1.0 and with the correlation distance equal to 20. The distance units are related to the size of the simulation area that is assumed to be 100 by 100 arbitrary units. The number of realizations is shown in the last column.

σ_G^2	μ_{LN} σ_{LN}^2 CV			**Correlation distance**		**n**
				40	**10**	
0.5	1.28	1.07	0.80	CASE 1	CASE 2	5000
1.0	1.65	4.67	1.31	CASE 3	CASE 4	25000

Figures

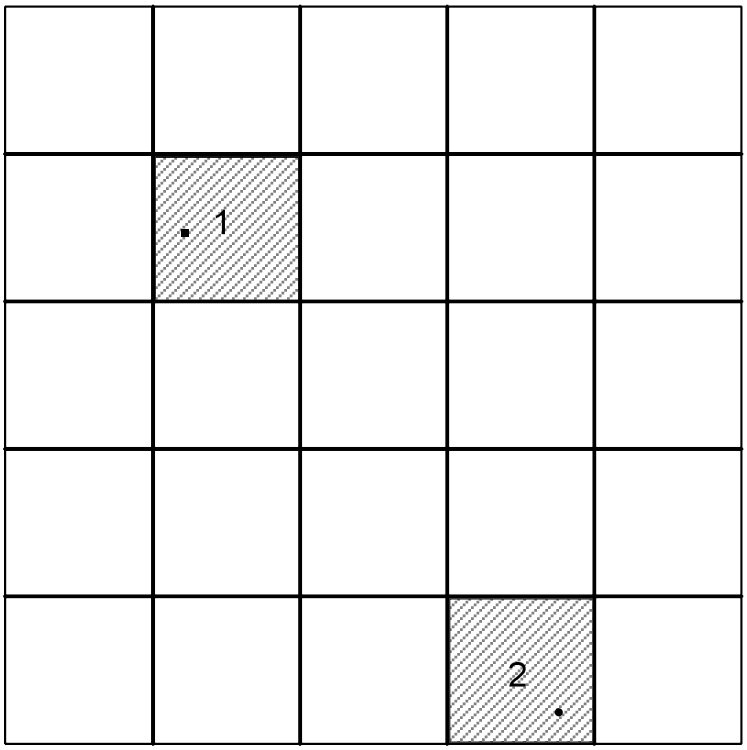

Figure 1: A schematic example of radar-rainfall grid with two pixels containing rain gauges (the hatched squares). The gauges are located randomly within the radar pixels.

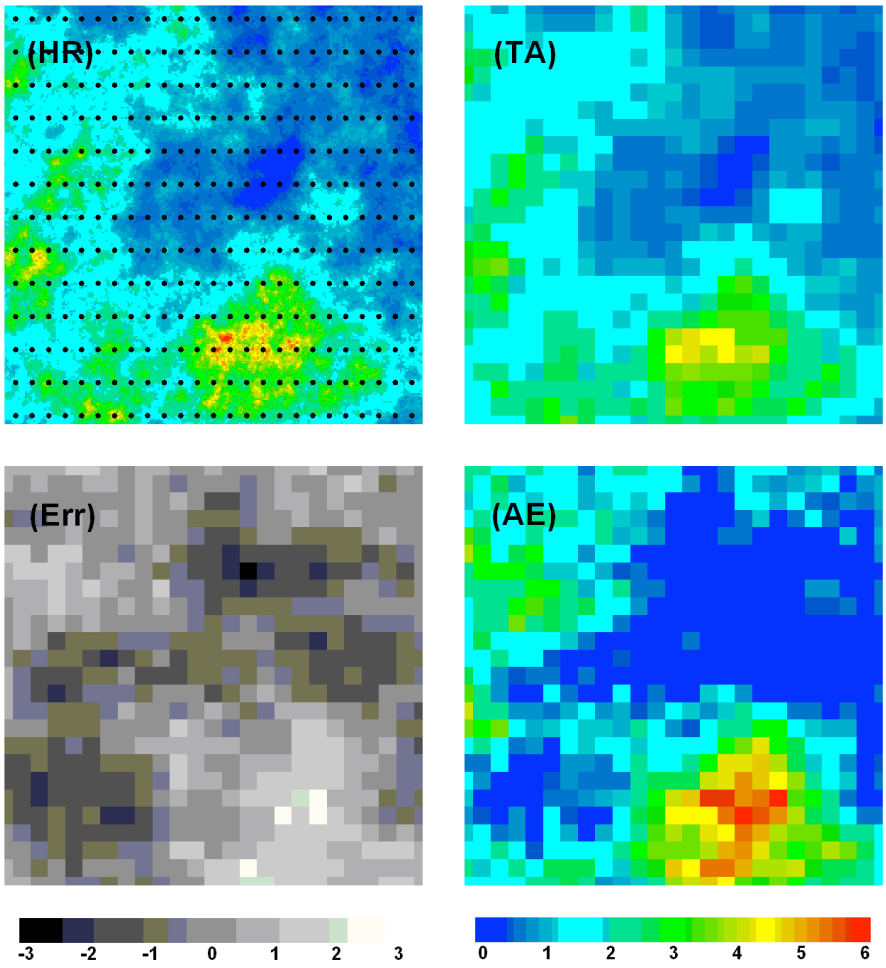

Figure 2: Example realization of four random fields: high resolution field (**HR**), true area averaged field (**TA**), error field (**Err**), and the "areal with error" (**AE**) field. The correlation distance of **HR** is d_{HR}=40, and its marginal distribution is lognormal with the mean equal to 1.65 and the coefficient of variation equal to 1.31. The **HR** panel also shows the sampling gauge network consisting of 325 (25 by 13) gauges. The error field (**Err**) is Gaussian with zero mean and a standard deviation equal to 1.0 and with the correlation distance of d_{Err}=20. The distance units are related to the size of the simulation area that is assumed to be 100 by 100 arbitrary units. The resolution of the **HR** field is equal to 0.4, and it is 4.0 for the remaining fields.

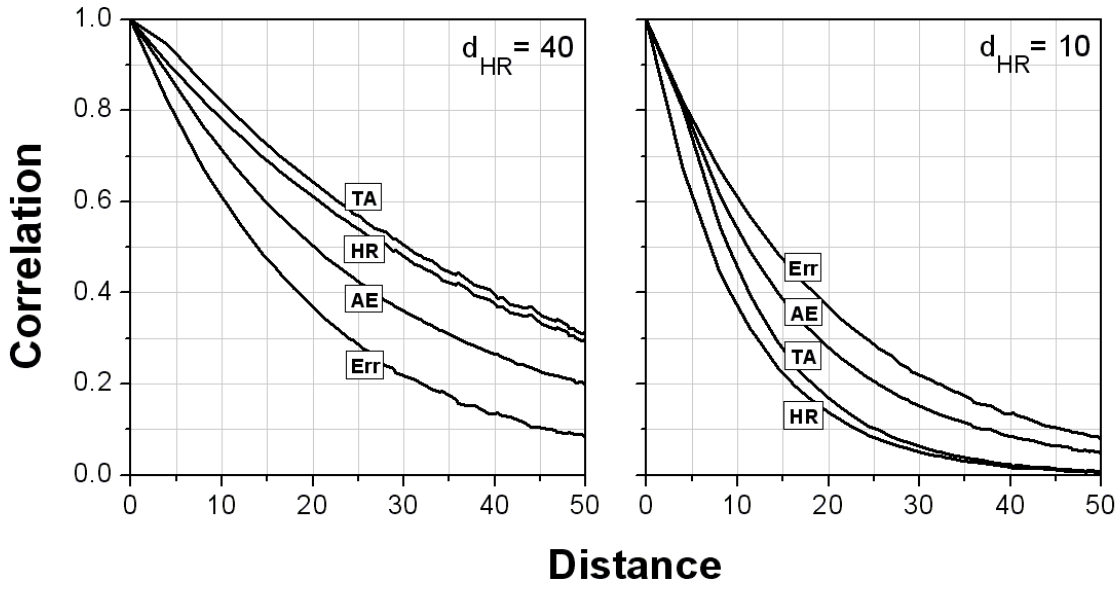

Figure 3: Correlation functions of the simulated high resolution (**HR**) Gaussian process, "true areal" (**TA**), error (**Err**), and "areal with error" (**AE**) processes estimated using the sampling network shown in Figure 2. The distance units and the parameters of the **Err** field are the same as in Figure 2.

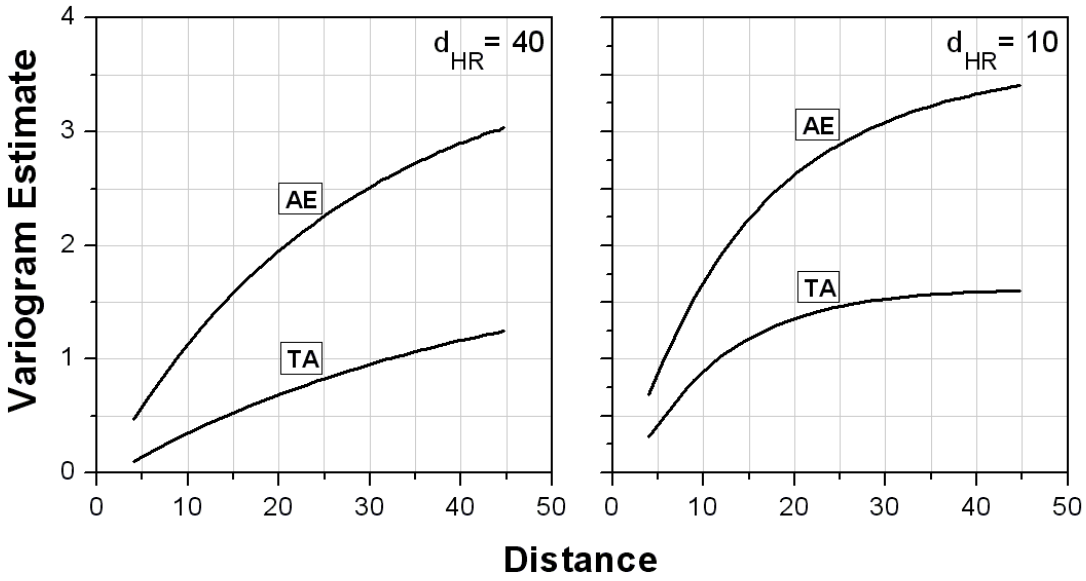

Figure 4: True areal (**TA**) and "areal with errors" (**AE**) variograms of the simulated Gaussian processes. The **AE** variogram is estimated using all the pixels available, and the **TA** variogram is obtained by integrating the variogram of the **HR** field. The distance units and the parameters of the **Err** field are the same as in Figure 2.

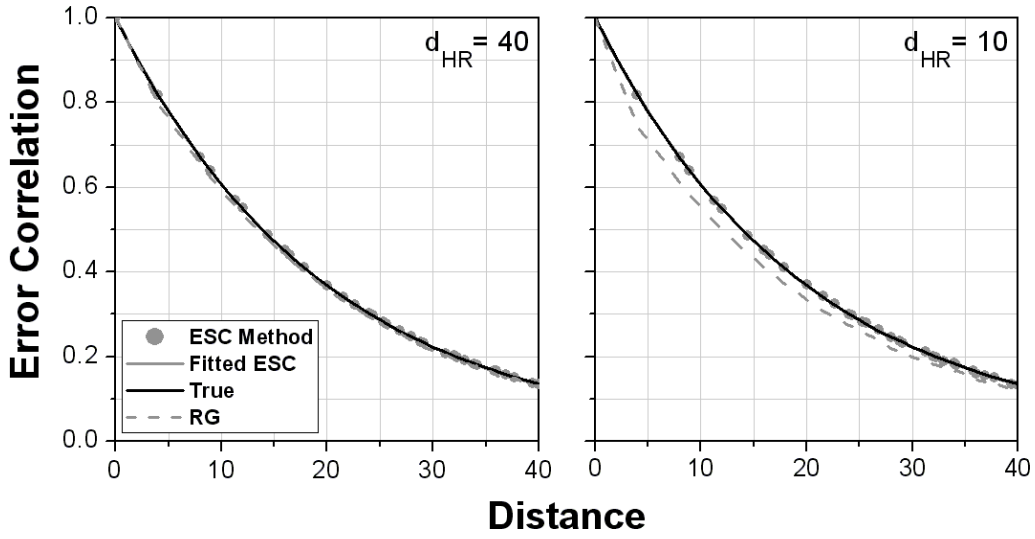

Figure 5: Comparison of three functions: 1) the estimated error spatial correlation (ESC) for Gaussian realizations corrected using our method, 2) the true ESC (with a correlation distance of 20) and 3) the spatial correlation structure of "radar-gauge" (RG) differences. The distance units and the parameters of the **Err** field are the same as in Figure 2.

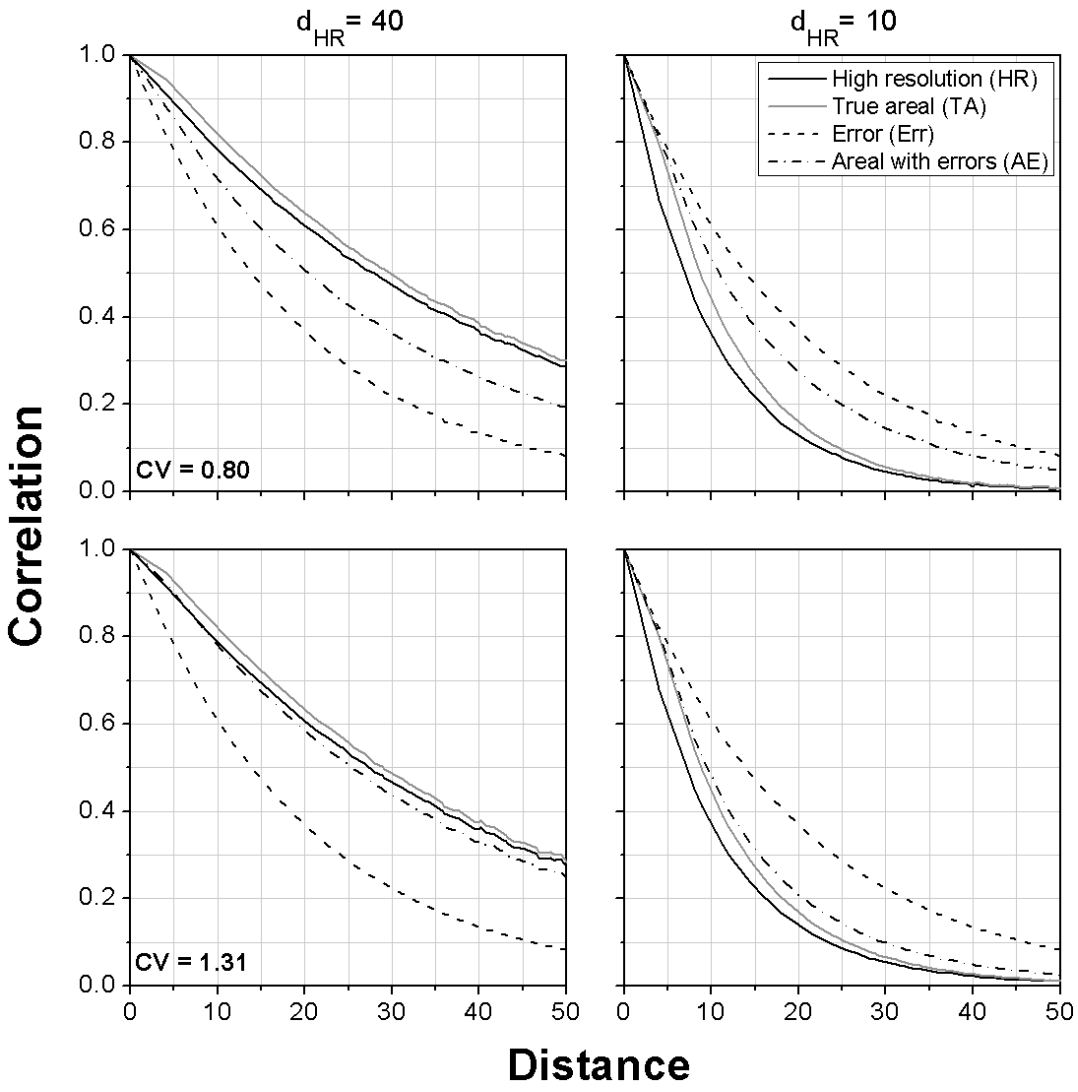

Figure 6: Correlation functions of the lognormal **HR** fields simulated with the parameters given in Table 1 and estimated using the sampling network shown in Figure 2. The distance units and the parameters of the **Err** field are the same as in Figure 2.

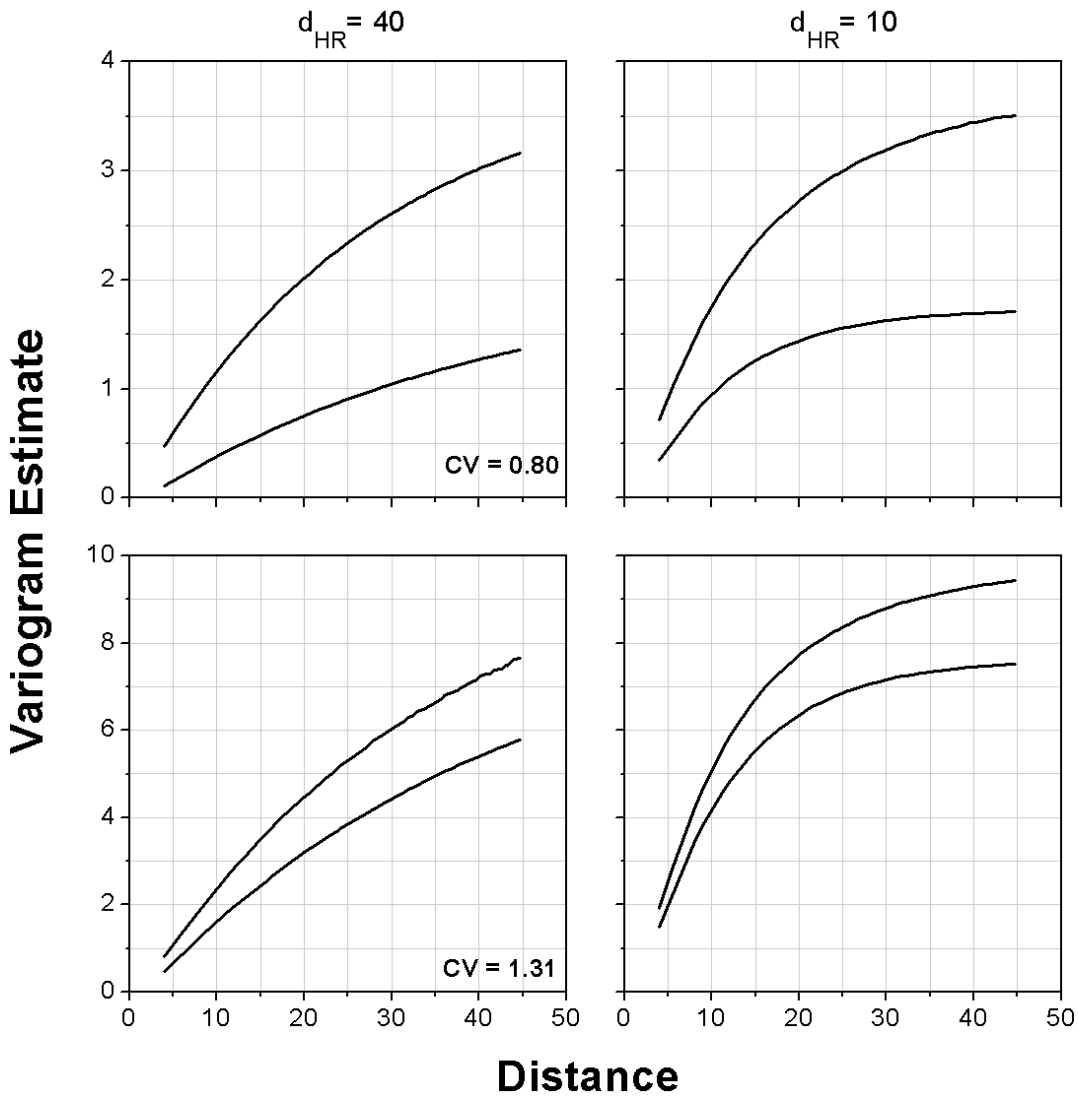

Figure 7: True areal (**TA**) and "areal with errors" (**AE**) variograms of the simulated lognormal processes of Table 1. In each panel, upper and lower curves are **AE** and **TA** variograms, respectively. The **AE** variogram is estimated using all the pixels available, and the **TA** variogram is obtained by integrating the point variogram. The distance units and the parameters of the **Err** field are the same as in Figure 2.

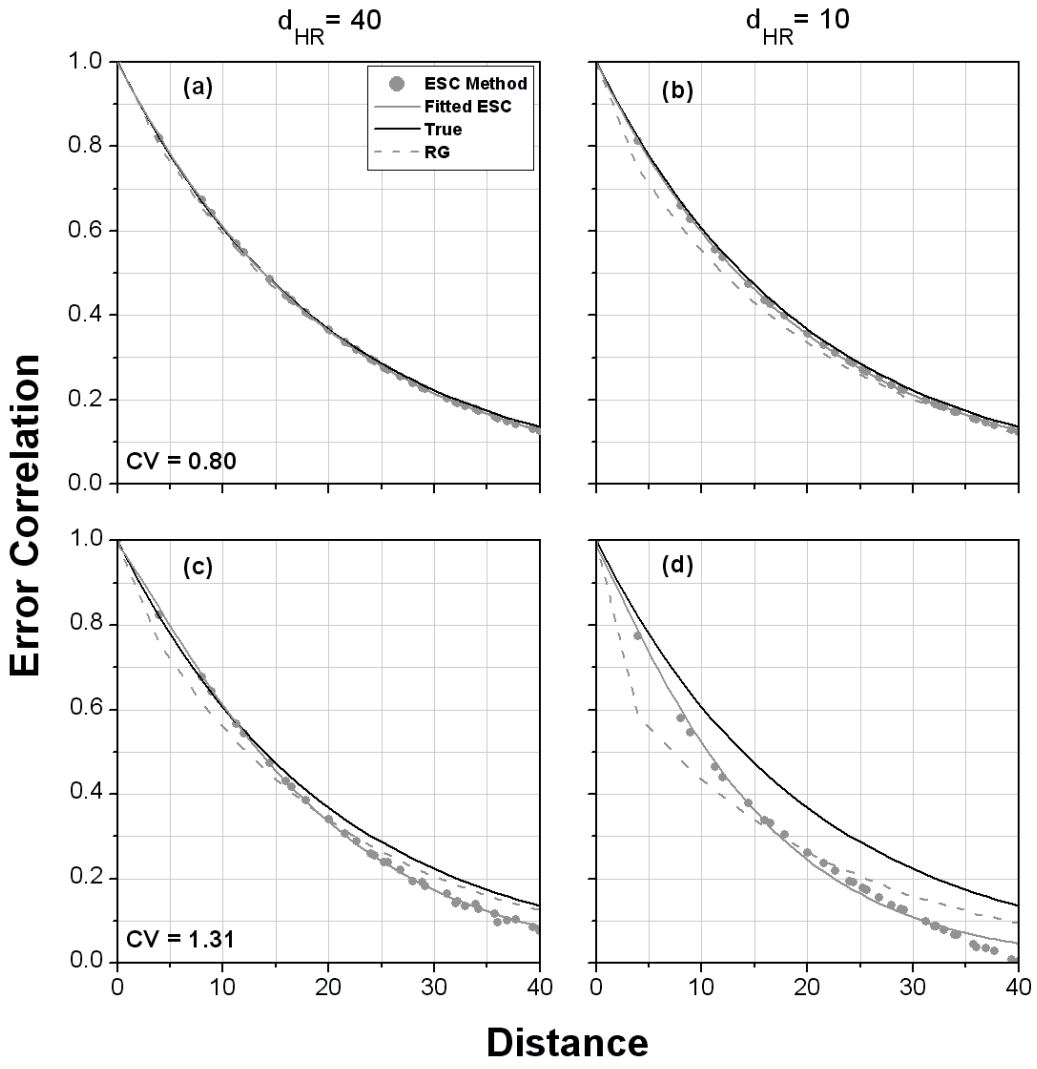

Figure 8: Comparison of error spatial correlation (ESC) for lognormal realizations retrieved using our correction method with the true ESC and with the spatial correlation structure of "radar-gauge" (RG) differences. The distance units and the parameters of the **Err** field are the same as in Figure 2.

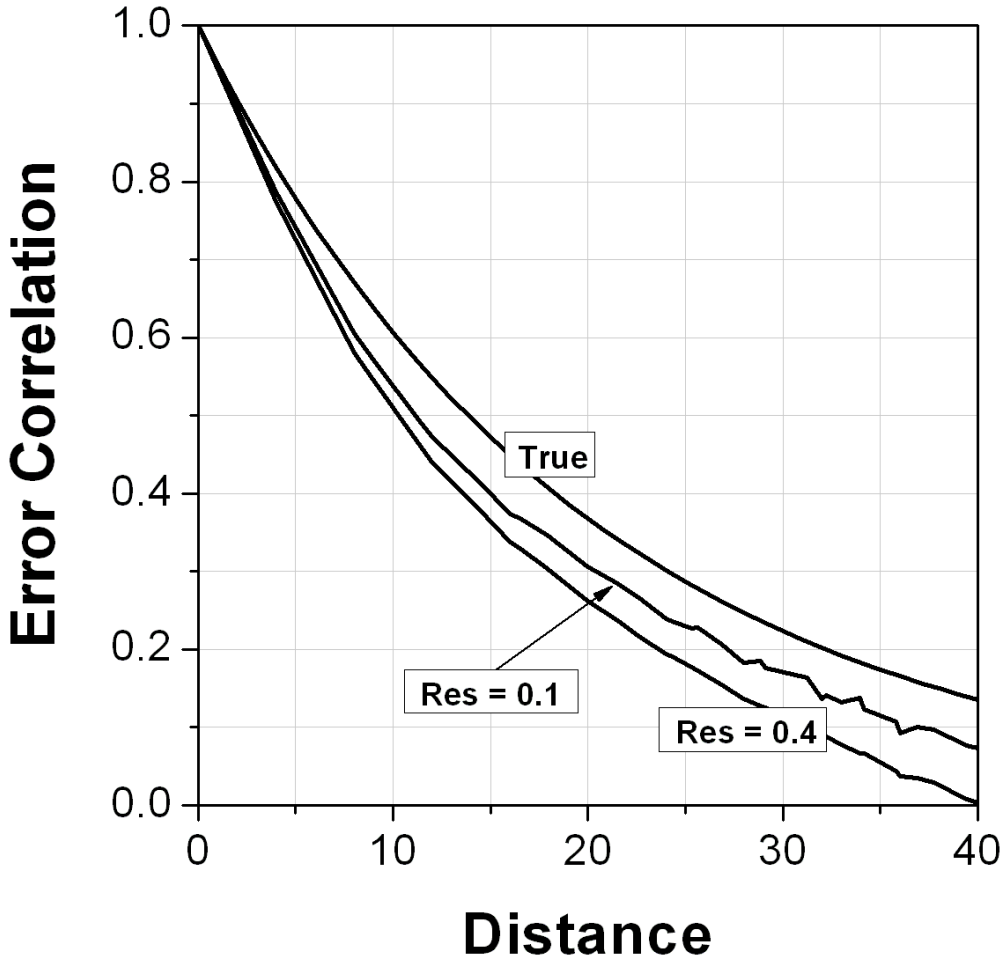

Figure 9: Sensitivity of the ESC method to the resolution (Res) of the simulation grid. The distance units and the parameters of the **Err** field are the same as in Figure 2.

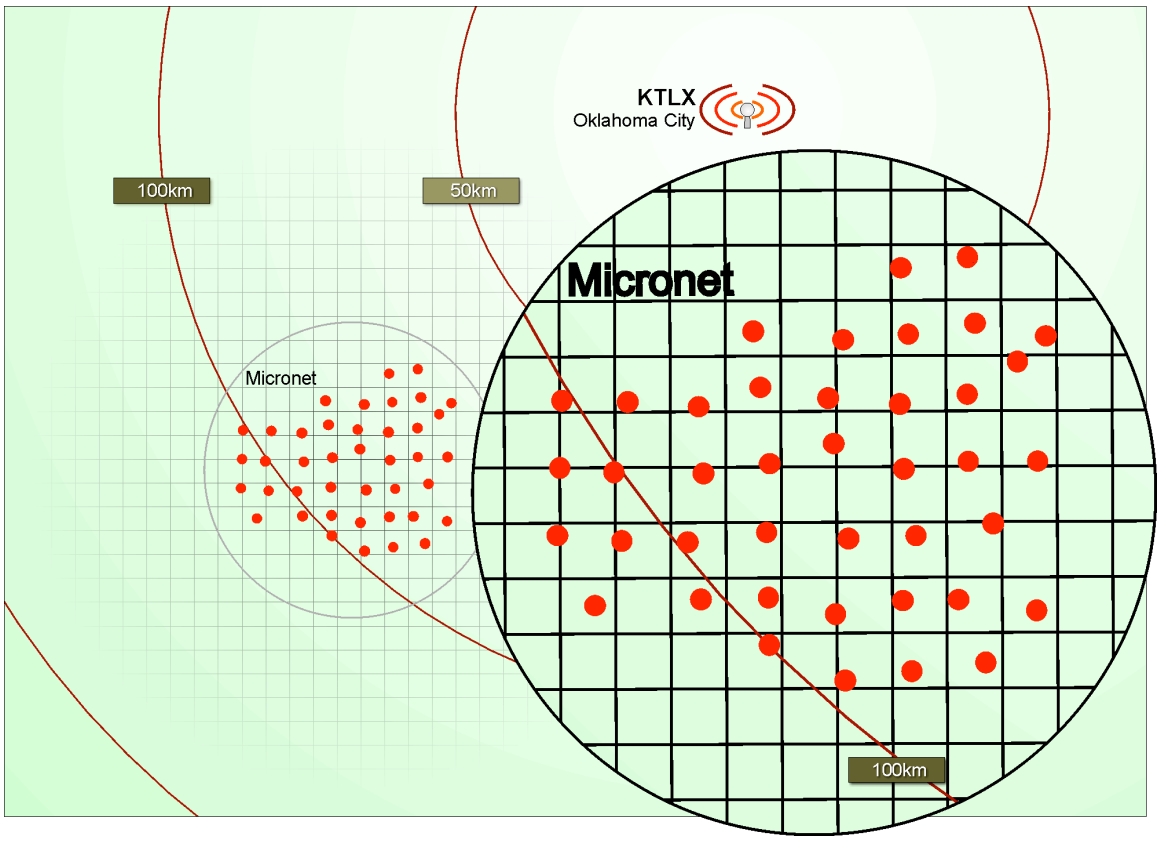

Figure 10: Map showing the location of the Oklahoma City NEXRAD (KTLX) radar site, Oklahoma Micronet, and HRAP grid.

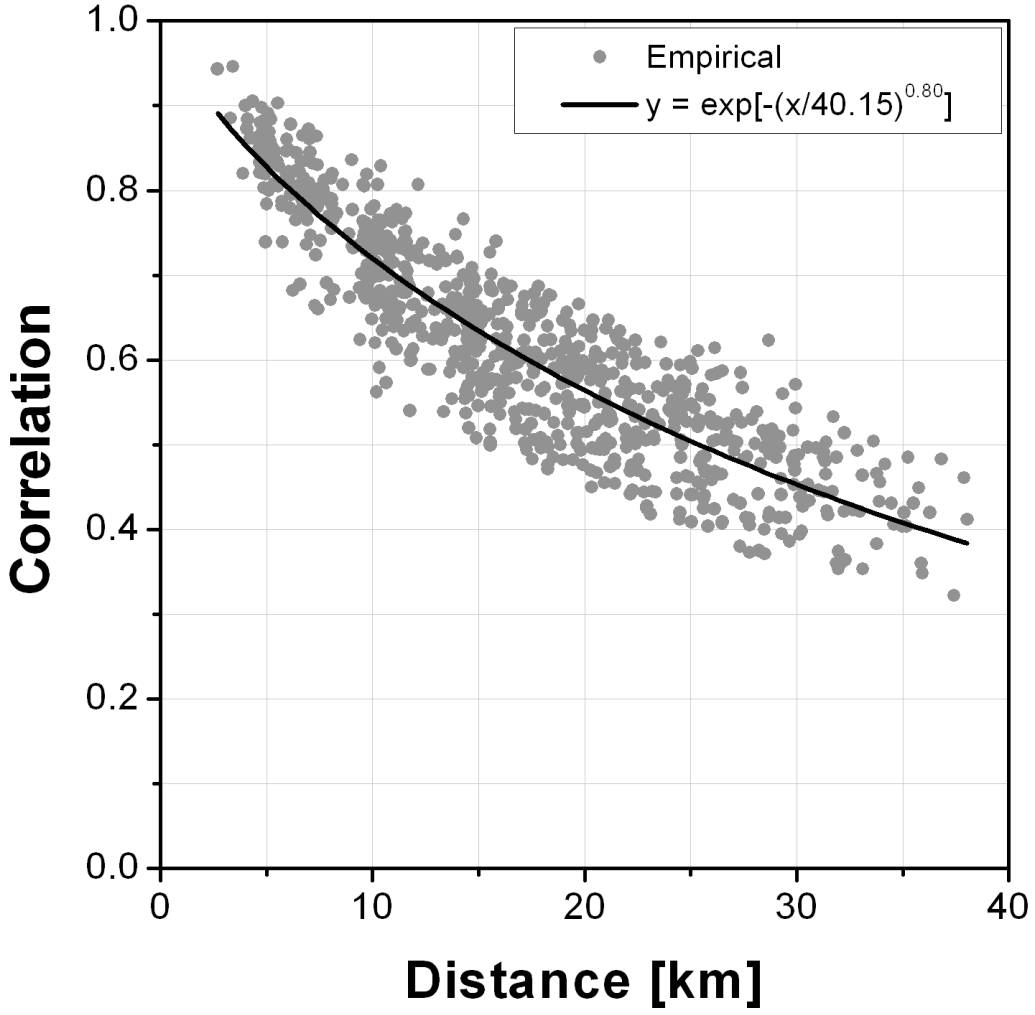

Figure 11: Pearson's correlation function of gauge-rainfall obtained using six years of warm season (April to September) rainfall data from Oklahoma Micronet.

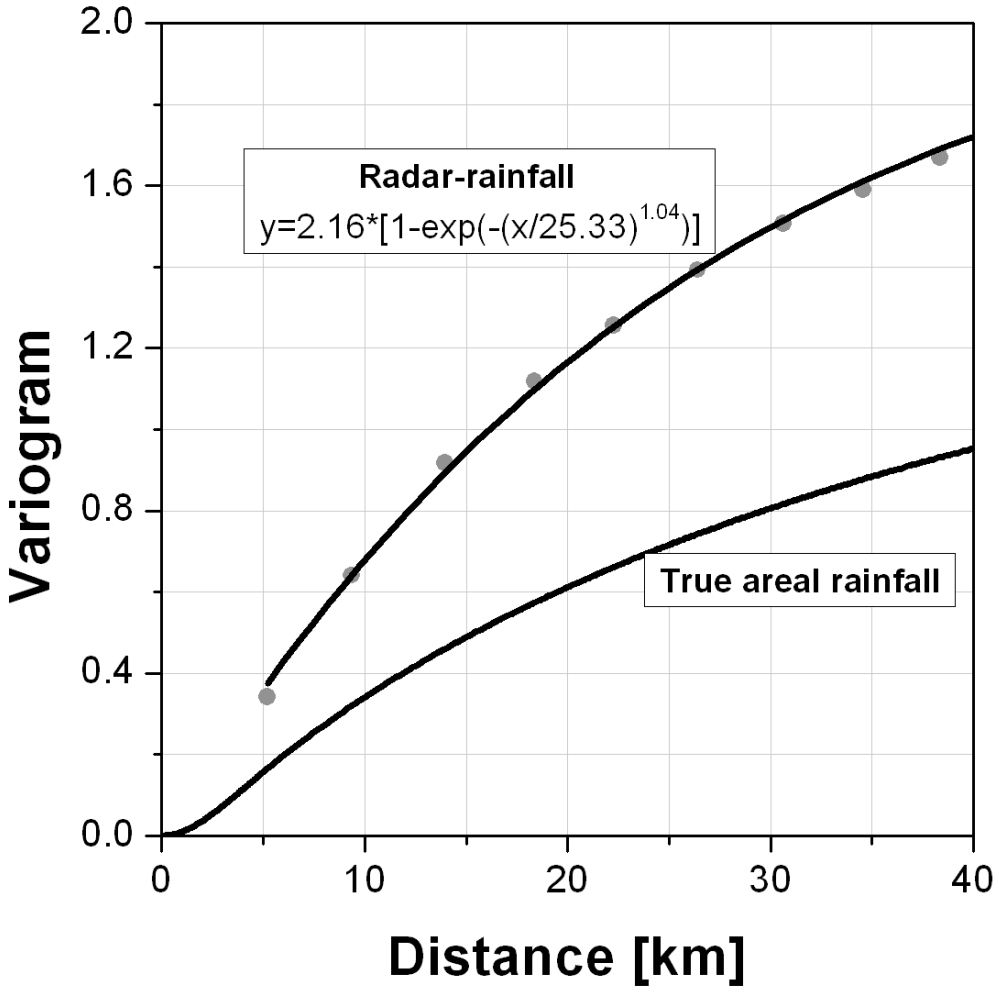

Figure 12: Radar-rainfall variogram for the National Weather Service's hourly digital product over the Oklahoma Micronet. The variogram of true areal rainfall is obtained by integrating the gauge-rainfall correlation function over the 4 km pixel.

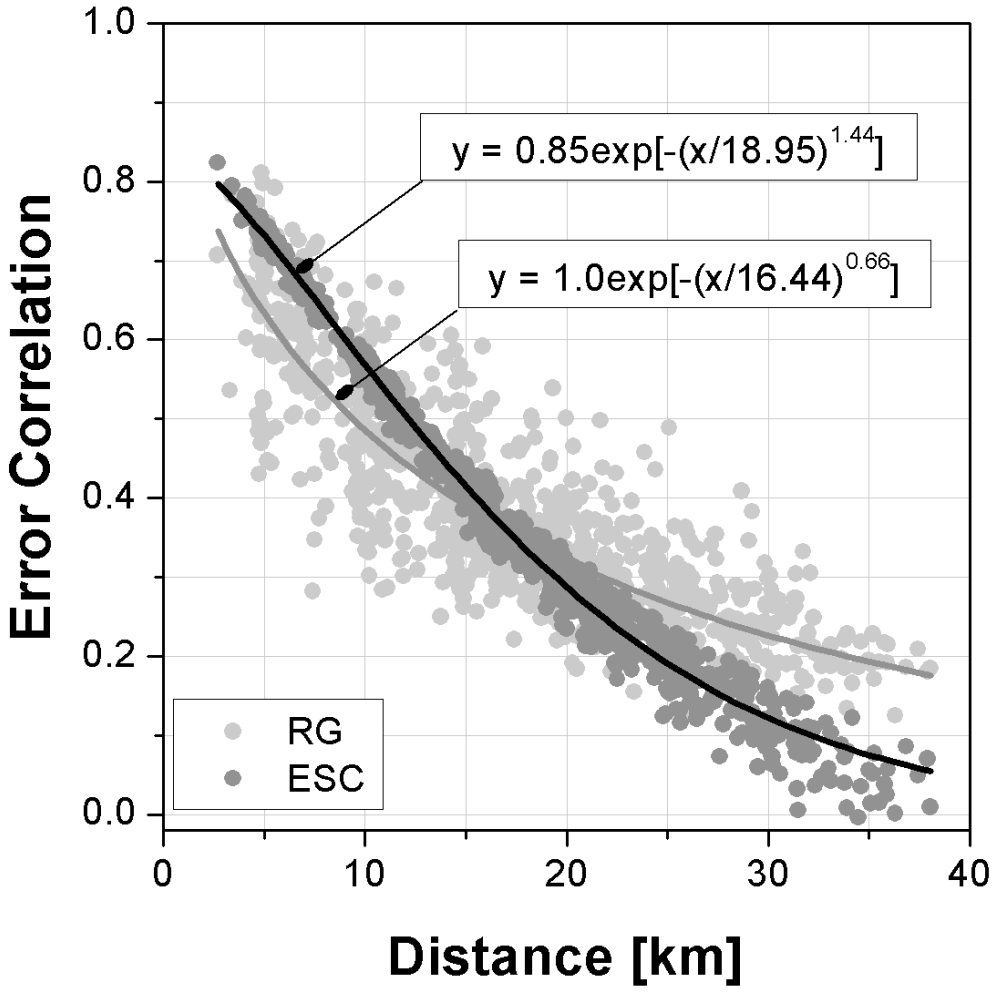

Figure 13: Comparison of error spatial correlation of the National Weather Service's hourly digital product with the spatial correlation structure of radar-gauge (RG) differences.